Communication

Quasi-line spectral emissions from high crystalline 1D Organic Nanowires

Ankur Sharma, Ahmed Raza Khan, Yi Zhu, Robert Halbich,
Wendi Ma, Yilin Tang, Bowen Wang, and Yuerui Lu

Nano Lett., **Just Accepted Manuscript** • DOI: 10.1021/acs.nanolett.9b02943 • Publication Date (Web): 11 Oct 2019

Quasi-line spectral emissions from high crystalline 1D Organic Nanowires

Ankur Sharma [1§], Ahmed Khan[1§], Yi Zhu[1], Robert Halbich[1], Wendi Ma[1], Yilin Tang[1], Bowen Wang[1] and Yuerui Lu[1*]

[1]Research School of Electrical, Energy and Materials Engineering, College of Engineering and Computer Science, the Australian National University, Canberra, ACT, 2601, Australia.

* To whom correspondence should be addressed: Yuerui Lu (yuerui.lu@anu.edu.au)

§ These authors contributed equally to the work.

ABSTRACT: Zero phonon line (ZPL) emissions have key applications in single photon emission sources, quantum information processing and single molecule spectroscopy. All recent attempts to realize ZPL emissions are based on the techniques of confining and doping molecules in matrices or solutions at low temperature-Shpol' skii systems. The requirement of two-component systems reduces the light emission efficiency from the molecules and limits their applications in solid state electronic applications and quantum computing devices. Here, we report the first experimental demonstration of Shpol' skii effect in a one-component organic solid-state system at low temperature. We observe a ZPL emission with width of ~1-2 nm and a high value of Debye-Waller factor (0.72) from our epitaxial grown high-crystalline and ordered 1D organic nanowire, which is attributed to specific molecular configuration and higher degree of orientation of molecules as compared to bulk thin film counterpart. Our results pave the way for organic 1D wires (with quasi-line spectra) for applications in lasing, nanosensors and interconnects/functional units in next generation miniaturized optoelectronics.

Keywords: Shpol' skii effect, organic nanowires, quasi-line spectra, crystallinity.

Introduction

Zero phonon lines (ZPL)[1] are narrow sharp peak emission at low temperature which are purely electronic in nature. They have characteristic vibrational structure and hence can be used for determining photophysical, photochemical and physicochemical properties of complex compounds.[2] Hence, there has been a tremendous revival of interest in narrow line-width emissions due to their fundamental applications in single photon emission sources, which have key applications in linear optics quantum information processing.[3] ZPLs have also been established to be applied for nano lasers,[4, 5] optical waveguides,[4, 6] flexible/cost-effective optical devices[7, 8] and tunable-wavelength emission displays.[9, 10], optical data storage[11] and processing in the space-frequency domain and single impurity molecule spectroscopy.[12] Zero-phonon or quasi-line spectral emissions were reported by Shpol' skii[13] in 1962 at low temperature by inducing the molecules in a matrix or solution at low temperatures, thus confirming the phonon less nature of these emissions.

There have been several attempts to generate similar quasi-line or Shpol' skii spectra emissions. Recently, self-assembled InAs quantum dots[3] and trapped atoms have been demonstrated as such sources for highly indistinguishable single photons and quasi-line emissions. Several complex polyatomic organic molecules embedded in molecular crystals or solutions have been demonstrated in the past to obtain ZPL emissions (See Table S1). But, all of them have been two-component systems which require the desired chromophore to be in a frozen solution or matrices in order to reduce the phonon sideband emissions. This dilutes the light emitting molecule concentration in the matrix and hence the light generation efficiency is considerably reduced.[2, 6, 7] There have been no reports so far which show a single component and single-crystal molecule solid-state system generating Shpol' skii spectra. Broad phonon sideband emission arises due to different energy level of molecules in a system[14] and that is why they need to be put in matrices or solutions as discussed above, to confine their degree of freedom

and achieve narrow quasi-line spectral emissions. In a single-crystal molecule system, high crystallinity is the key to observe Shpol' skii effect but until now it has been a challenge to grow highly crystalline solid states systems that generate ZPL emissions. One-dimensional (1D) nanostructures such as nanowires, nanoribbons/belts and nanotubes have gathered significant attention due to their two dimensional quantum confinement.[7, 15] This makes them promising candidates for achieving quasi-line spectral emissions. But most those nanomaterials have been mostly externally doped conjugated polymers[16-18] or large two dimensional non-linear extended aromatic systems like hexabenzocoronene.[15, 19] That makes it difficult to achieve large scale high order crystalline and defect free growth of 1D structures, especially with molecules that show π–π face stacking necessary to make 1D structures.[19, 20] Most of the reported 1D organic structures have been demonstrated in liquid phase[21, 22] grown by using self-assembly in liquid phase solutions, restricting their applications in solid state electronic devices.[23] Low molecular weight organic materials on the other hand offer a distinct advantage as compared to their inorganic counterparts in terms of their good processability,[24] large-scale/low-cost synthesis,[7, 19] high photoluminescence (PL) efficiency[25] and molecular tunability of electronic properties.[26, 27]

But, in solid state growth of organic molecules over a substrate, it is difficult to achieve dimensionality control and effectively control the width and length of the 1D nanostructure.[7, 19] Moreover, it is well known that in organic crystalline structures the opto-electronic and electronic properties are a direct function of the molecular orientation, degree of crystallinity and defect states in the lattice.[28, 29] For ensemble organic molecular systems in solution, the local arrangement of the molecules in the solution affects their ability to absorb light and hence affects their optoelectronic properties.[30] There have been recent reports on using physical vapor deposition (PVD)[9, 10, 14, 31] techniques to grow solid states 1D crystalline organic structures. However, they still have not been able to control monodispersity of the organic molecules,

especially with low-molecular weight organic molecules as deposition sources.[7, 19]

Here, we present a single component, high crystalline organic 1D nanowire made from single-crystal low molecular weight oligoacene- pentacene (PEN) molecule deposited on hexagonal boron nitride (hBN) using a low temperature PVD process. We report interesting optical properties form the 1D nanowires at room and low temperature. The PL spectra from the nanowires is clearly resolvable into three vibronic peaks at room temperature as compared to the broad sideband emission from bulk thin film pentacene. We attribute this PL spectra to a high degree of crystallinity and reduced degrees of translational and rotational freedom[32] of molecules in 1D PEN wire. Hence, resulting in clearly resolvable vibronic energy levels and reduced charge-phonon coupling in the lattice. At cryogenic temperatures, due to further freezing of molecular degrees of freedom and reduction of thermal phononic coupling results in quasi-line spectra[33] from PEN wires. This emergence of these atomic-like quasi-line spectra is called Shpol' skii effect[13, 34] and was reported in frozen organic solutions at low temperatures by Shpol' skii in 1952. The reported quasi-line spectra have a linewidth of ~1-2 nm and are a resultant of the reduced phononic coupling with the excitons in the lattice[2]. The linewidth reported in our case is much lower as compared to the linewidth reported from similar organic 1D nanostructures[14] grown using similar PVD methods. These quasi line spectra arising at low temperatures are ZPLs[2] attributed to zero-phonon transitions between the electronic energy levels of the organic molecules, confirmed by a high value of the Debye-Waller factor (*DW*).[2, 33] We further establish the high crystallinity and higher degree of molecular orientation of the PEN molecules in the 1D nanowire structure using polarization-resolved PL emission spectra and time-resolved PL emission. We also demonstrate a metal oxide semiconductor (MOS) device incorporating the 1D PEN wire to effectively demonstrate an external electric control of the quasi line spectral emission at low temperatures. Our results effectively demonstrate the

use of PEN 1D organic nanowires for future optoelectronic devices such as nanolasers[35], OFETs[36], multi-colored light emitting diodes (LEDs)[10], optically driven lasers[37], photodetectors, logic gates and construction of interconnects and functional units of next generation miniaturized optoelectronics.[7]

Results and Discussion

Among light-weight oligoacenes, pentacene and its derivates have shown best performances in thin-film devices[38]. Thus, we chose pentacene for our 1D growth. Figure 1a shows the optical image of the PEN wires grown on hBN substrate. hBN provides a defect free and dangling bond free flat area for molecular deposition with high degree of molecular orientation[39]. Mechanically exfoliated few-layer hBN sheets were transferred onto a 285 nm SiO_2/Si substrate. The PEN was then deposited using a thermal vapor deposition process using a tube furnace (Figure S1). (See Methods and Supplementary information Note 1). The grown PEN wires were characterized using Raman spectroscopy (Figure S2). The growth of the PEN wires was optimized at various growth temperatures (Figure S3a) and time durations (Figure S3b) to achieve long length and high crystalline 1D nanowires. High resolution AFM imaging was used to characterize the physical thickness and diameter of the PEN wires (Figure 1b). Most of the PEN wires had a circular cross-section with an average width of ~300-400 nm and an average thickness of ~250-300 nm. The average length of the wires was ~14 μm, which is much higher than previously reported PVD grown 1D nanowires on substrates[7, 10, 14]. Figure 1c shows the schematic growth mechanism of 1D PEN nanowires on hBN substrates. First, the smaller PEN molecules are connected linearly by H-bonds forming long chains and depositing over hBN surface utilizing $\sigma-\pi$ interaction with the substrate[39]. The vertical deposition then is a result of van der Waals interaction between pentacene molecules. At this juncture, as the deposition rate increases, $\pi-\pi$ interactions between PEN molecules cause the molecules to

bend inwards facing each other[7] leading to the formation of wire like 1D structures. We confirmed the same using high resolution SEM imaging (Figure 1d).

The prepared samples were then excited using a 532 nm CW laser. The resultant PL emission spectra is shown in Figure 1e. The PL spectra from the 1D PEN wire is clearly resolved in to three peaks at 600 nm, 660 nm and 730 nm. The origin of the peaks is explained later. The spectrum from 1D PEN wires is in sharp contrast to the broad and much weaker PL emission from thin film pentacene grown on the same substrate and bulk pentacene samples. The optical absorption and emission from organic molecular assemblies is a direct function of the molecular crystallinity and degree of orientation[29]. Hence, well resolved and high-intensity PL emission from 1D wires is a resultant of the highly crystalline an ordered growth of PEN wires on a clean defect free flat hBN adsorption surface. To further confirm the role of hBN in achieving ordered growth, we ran the growth of PEN wires again using the same methods and conditions on a SiO_2/Si substrate. We observed tiny needle like 1D structures protruding out of micelle like nucleation sites (Figure S4). The growth of those 1D PEN structures on SiO_2 was highly disordered and the PL emission (Figure S4c) were much weaker and less resolved as compared to the wires grown on hBN. Thus, establishing the role of hBN as a template or adsorbent surface for the ordered high crystalline and dimensionality controlled growth of 1D PEN wires.

Shpol' skii effect and quasi-line spectra

To further understand the optical properties of crystalline 1D PEN wires and substantiate their role for various optoelectronic applications, we performed temperature dependent PL spectroscopy down to 77 K. Figure 2a shows the PL spectra from 1D PEN wires at various temperatures. The spectra start to resolve into various sharp and narrow linewidth peaks as the temperature decreases. The first emergence of narrow peaks is spotted at 213 K (Figure S5).

At 77 K, the spectrum is clearly resolved into sharp quasi-line emission peaks with an average line width of 2-3 nm (See Table S2 for fitted peak positions). In some optimal growth cases, we observed the line-width to be ~ 1nm (Figure S6). Whereas, we did not observe such narrow linewidth PL peaks from 1D needles grown on SiO_2 (Figure 2b). The emergence of quasi-line spectra from 1D PEN wires is very different from the broad sideband PL emission from thin film PEN grown on similar hBN substrate (Figure S7).

The origin of quasi-line spectra from 1D PEN wires and the difference with thin film PEN be explained using the energy level band diagram in Figure 2c. In bulk thin films of organic molecules such as pentacene, the emission band broadening/dispersion results mainly from the fact that various molecules have different energy levels[40]. As a result, multiple vibronic band are formed (also called Davydov splitting[41]). The energy levels (in both ground and excited states) are roughly divided in vibronic sub-bands, defined by the number of quanta υ (=1,2…). Each vibronic band has further vibrational sub-bands induced due phononic coupling of charges (indicated by $\tilde{\nu}$=1,2...) The width of each vibronic band incorporating molecular interaction and vibrational frequency of molecules has been theoretically calculated by Spano et al.[42] Due to low crystallinity, the charges couple with phonons (vibrations) in the crystal lattice plane to form diffused vibronic/vibrational bands (as shown Figure 2c). Each vibrational band is spread due to this strong phononic coupling of rotational translational states of charges[2]. The interaction of molecules with lattice phonons is represented by spread of vibrational sublevels. Multiplicity of characteristic vibrational and vibronic bands of these molecules results in further diffusiveness of electronic-vibrational bands and causes a quasi-continuum spectrum as obtained from bulk thin films. The inhomogeneous spectral broadening arises from electronic transitions involving lattice phonons, giving rise to a comparatively broad phonon sideband emission (PSB)[2, 32].

In our single crystalline, 1D PEN wires due to flat h-BN substrate, the molecules are confined

distinctly in the lattice with a specific geometric configuration and higher degree of orientation[4, 6, 7, 14] as compared to bulk organic thin films, with less defect and interfacial states. This limits the large rotational and translational degrees of freedom of molecules and this ordered environment drastically reduces the phonon coupling resulting in narrower optical transitions[2]. Even at room temperature narrowing of vibrational level occurs, simplifying the optical spectra into discrete narrower emissions (Figure 1e). The emergence and enhancement of vibrational structures can be attributed the increases of long-range order and higher degree of molecular orientation in PEN wires.

At low temperature all vibronic transitions can be further resolved (with FWHM ~ 2-3 nm), resulting in an almost quasi-line spectrum called the Shpol' skii effect. At low temperatures, the degrees of freedom for the molecules are further frozen resulting in further educed electron-phonon coupling. This causes the PL spectra to be resolved in to quasi-line peaks or the narrow zero-phonon lines[43] (ZPL) emissions from the vibronic/vibrational sub bands to ground state (as shown in Figure 1c). Such line-spectra only appears upon specific transitions in the band structure, which do not involve lattice phononic vibrations (analogous of Mössbauer[44] lines). The reduction in spread of vibronic/vibrational sub bands occurs due to high ordered growth of PEN molecules over hBN and further reduction in phonon-electron coupling at low temperature. It has been shown in the literature that Shpol' skii effect is affected by guest-host molecular interactions[31, 32]. Hence, the emergence of Shpol 'skii spectrum can be attributed to these two factors: highly ordered molecular orientation (high crystallinity) and low temperature. ZPLs were not observed from the PEN needles on SiO_2 (Figure 2b). This further substantiates the role of high crystallinity in PEN wires in achieving ZPL spectral emissions at low temperature.

It has been shown theoretically that the electron-phonon coupling and change of temperature influences the FWHM and integrated PL emission from organic matrices[33, 38]. To further

confirm the Shpol' skii effect and the role of ZPLs in the spectra obtained from 1D PEN wire, we performed temperature dependent FWHM and Integrated PL intensity analysis. The relation between the integrated intensity of the ZPL and total intensity of the (ZPL+PSB) band is determined by linear-electron phonon coupling and is called Debye-Waller factor (*DW*)[2, 45] and is defined by the following equation (1).

$$DW = \frac{I_{ZPL}}{I_{ZPL} + I_{PSB}}$$

where, I_{ZPL} is the integrated PL intensity from the sharp zero-phonon line peak and I_{PSB} is the total integrated area of the remaining broad sideband emissions. The I_{ZPL} and I_{PSB} were obtained by fitting the PL spectra from PEN wires using a Lorentzian fitting function (Figure S8) and then the integrated area under the curve under the sharp peak I_{ZPL} and under the nearest phonon sideband emission I_{PSB} were obtained to determine the *DW* factor

The variation of extracted *DW* factor from 1D PEN wire as a function of temperature is shown in Figure 2d. The high value of DW factor (0.72) at 77 K confirms the limited phonon coupling with the charges resulting in quasi-line spectra. As a comparison we have also shown calculated *DW* factor for an excitonic emission from 1L WSe_2 monolayer. The linewidth of PL emission peak is also a direct function of phonon coupling. Figure 2e (Figure S9) shows the variation in full-width half maximum (FWHM) from peak 1(peak 2, 3) emissions from 1D PEN wire and 1L WSe_2 monolayer. The FWHM from 1D PEN wire is much lower as compared to the excitonic peak width at 77 K from 1L WSe_2. The sharp reduction in FWHM (~ 2-3 nm at 77 K) from the PEN wire PL peak 1, confirms the reduced phonon coupling in the PEN crystal lattice[46] resulting in quasi-line spectral emissions, which is consistent with previously reported ZPL emissions from low dimensional organic materials[2] and other Shpol' skii matrices (See table S1). We further performed pumping power dependent PL measurements at 77 K (Figure S10), which confirmed the mission to be below lasing threshold.

High order crystallinity and molecular orientation

To further understand the crystalline structure and orientation of pentacene molecule unit cells inside the 1D PEN wire, we performed polarization angle resolved PL emission spectroscopy at both room temperature and 77 K. Figure 3a shows the PL spectra at various emission polarization angles at room temperature. PL intensity from 1D PEN wires strongly depended on the emission polarization angle θ and showed a period of 180 degrees. Peak 1 (600 nm) showed opposite polarization dependence as compared to peaks 2 (660 nm) and 3 (730 nm). Based on the polarization data and theoretically predicted π–π[47] molecular packing in pentacene[38], we can identify the crystal faces in PEN wire as shown in Figure 3b. The wires grow along the 010 axis or the 100 face[19, 31] (see inset SEM image in Figure 3b and Figure S11). Figure 3c shows the polar plot of PL intensities as a function of polarization angles. Peak 1 is clearly polarized along the long'b' axis of PEN unit cell, while peak 2 and 3 are aligned along the 'a' axis[31]. This clearly highlights anisotropy in 1D PEN wires originating due to high crystalline and ordered growth in the 1D wires. We performed similar polarization resolved (excitation and emission) measurements at 77 K (Figure 3d and Figure S12) to understand the anisotropic behaviour of the Shpol' skii spectra observed at 77 K. We observed the same trend as at room temperature. The quasi-line spectra peaks 1 and 2 (See Table S2) are aligned along the 'b' axis (Figure 3e). The remaining quasi-linear peaks were aligned along the 'a' axis of PEN unit cell as shown in Figure 3f and Figure S13.

Increased crystallinity and order can also lead to enhanced lifetime of PL emission peaks in crystalline materials[48, 49]. To substantiate the high crystallinity in our 1D nanowires, we also performed time-resolved PL (TRPL) measurements at room temperature and 77 K. Figure 4a shows the decay curve obtained from peaks 1,2 and 3 from PEN 1D wire at room temperature and the bulk thin film. The decay trace curves were deconvoluted with respect to the instrument response function (IRF) and then were fitted using the equation: $I = A\, exp(-\frac{t}{\tau 1}) + C$, where

I is the PL intensity, A and C are constants, 't' is time, and τ_1 is decay rate indicating emission lifetime. The long single exponential lifetime represents radiative recombination time at room temperature.[50] An effective lifetime of $\tau_1 = 3.36 \pm 0.6$ ns, 3.07 ± 0.3 ns and 2.74 ± 0.4 ns (Figure 4c) was extracted for peaks 1, 2 and 3 respectively at room temperature, which is about three times higher than the extracted radiative lifetime form thin film pentacene of 1.24 ns. Similarly, at 77 K, effective radiative lifetime for 5 major peaks was extracted as shown in Figures 4b, d. The error bar in Figure 4c, d shows the variation in the measured data from around 20 similar samples that were tested over a period of few weeks. The effective lifetime from 1D PEN wire increased to an average ~ 4.5 ns (Figure 4d) while the thin film lifetime was reported to be around 1.01 ns. It is important to note here that the prolonged lifetime in PEN wires as compared to thin film pentacene is due to the lower trap density and lower degree of non-radiative trap/defect assisted recombination of excitons as compared to the thin films. Similar effects have been observed in other crystalline low dimensional material such as TMDCs and perovskites[51, 52]. Thus, establishing the high order crystallinity and high degree of molecular orientation in our 1D PEN nanowires.

MOS device based on 1D PEN nanowires

We further incorporated the 1D PEN nanowire into a metal-oxide semiconductor (MOS) device to use external static back gate voltage to manipulate the quasi-line spectra for various optoelectronic device applications. Figure 5a shows the schematic diagram of the MOS device used for back gate voltage dependent PL modulation. During the measurements, the gold electrode was grounded, and the p+ doped Si substrate was used as a back gate providing a uniform electrostatic doping for the 1D PEN in this MOS device. The measured PL spectrum was very sensitive to the electrostatic doping and can be significantly modulated by the gate voltage. The PL intensity decreases when we inject negative charge into the samples, indicating

that the 1D PEN has an initial n-type doping, Figure 5b(c) shows the variation in PL spectra at different back gate voltages at 298 K (77 K). The variation in PL intensities with back gate voltage is evident even for quasi-line spectra peaks at low temperature. The variation in PL intensity of peaks 1, 4 and 12 (See Table S2) as a function of back gate voltage is shown in Figure 5d. Electrostatic control of the quasi-line spectra is further demonstrated through change in *DW* factor as a function of back gate voltage (Figure S14 and S15). Thus, establishing the applications of 1D PEN nanowires in future optoelectronic device applications.

Conclusion

In conclusion, we have demonstrated a quasi-line spectrum from a single component, solid state system of low-molecular weight single crystalline molecule organic material. We experimentally observed zero-phono lines in the PL emission spectra from 1D PEN nanowires originating due to Shpol' skii effect at cryogenic temperatures, which have not been reported before from single molecular crystalline solid-state systems. This was achieved due to a highly crystalline and ordered growth of PEN molecules in a 1D nanowire grown over an adsorbent defect free and flat hBN surface. Control of dimensionality and order in PVD process has been a challenge to grow similar 1D organic nanostructures for various optoelectronic applications. We demonstrated an optimized 1D nanowire which has high crystallinity and subsequently exciting optical properties for future optoelectronics. The restriction in degrees of freedom and reduced electron-phonon coupling in 1D nanowires led to vibronically well-resolved PL spectra. At low temperatures, further thermal phonon coupling is reduced, and the PL spectra is resolved in to quasi zero-phonon lines- the Shpol' skii spectra, as evident through extracted FWHM and *DW* factors form temperature dependent measurements. We further establish the high crystallinity through angle and time-resolved PL measurements. We finally demonstrate a MOS device based on 1D PEN nanowires, which shows an external control of quasi-line spectra using back gate voltage. Our results pave the way for use of organic 1D nanowires in nanolasers, OFETs, optical waveguides, chemical sensors, photodetectors and functional/interconnecting units of future nano optoelectronic and photonic devices.

Methods

Material growth: h-BN flakes were mechanically exfoliated onto a thermally grown 285 nm thick SiO_2 layer deposited over silicon substrate. Before physical vapor deposition (PVD), optical microscope was used to characterize the topological information. The pentacene (purchased from Chem Supply: P0030-1G) was then deposited over the h-BN flakes, kept centered in a vacuum tube in the furnace. h-BN sheet on SiO_2/Si substrate was placed around 15 cm downstream and a molecular pump was used to evacuate the quartz tube to ~10^{-4} mbar. The furnace was heated up to 135-185°C for various time intervals to grow PEN wires. (See S.I. Note 1). Then, the whole system was naturally cooled down to room temperature under vacuum. All the samples were characterized, and layer thickness were identified using the standard AFM measurements, which were collected in ambient atmosphere at room temperature with a Bruker Multi-Mode III AFM. For the MOS structure, used for back gate-dependent PL measurements, we transferred the 100 nm thick gold electrode to contact part of the 1D PEN nanowire as the probing pad. The voltage was supplied using a Kiethly 4200 semiconductor analyzer.

Optical Characterization: PL measurements at room temperature and 77 K were conducted using a Horiba LabRAM system equipped with a confocal microscope, a charge-coupled device (CCD) Si detector, and a 532 nm diode-pumped solid-state (DPSS) laser as the excitation source. The laser excitation spot was 0.5 μm in size calibrated using pinhole and confirmed using direct CCD imaging technique. The laser power excitation density was 525.5 W/cm^2 unless otherwise specified. The laser beam was gaussian in nature and was focused on the middle cross-section of the wire for all measurements. For temperature-dependent (above 77 K) measurements, the sample was placed into a microscope-compatible chamber with a low temperature controller (using liquid nitrogen as the coolant). In the experiment, the incident polarization angle was controlled by an angle-variable half-wave plate and was fixed, and the

polarization angle of the emission (θ) was determined by using an angle-variable polarizer located in front of the detector. Time resolved PL measurements were conducted in a setup which incorporates μ-PL spectroscopy and a time-correlated single photon counting (TCSPC) system. A linearly polarized pulse laser (frequency doubled to 522 nm, with 300 fs pulse width and 20.8 MHz repetition rate) was directed to a high numerical aperture (NA= 0.7) objective (Nikon S Plan 603). PL signal was collected by a grating spectrometer, thereby either recording the PL spectrum through a charge coupled device (CCD; Princeton Instruments, PIXIS) or detecting the PL intensity decay by a Si single-photon avalanche diode (SPAD) and the TCSPC (PicoHarp 300) system.

Author Contributions

Y. L. conceived and supervised the project; A.K. and Y. Z. prepared pentacene samples; A. S. carried out all the optical measurements; A. S, Y. L. and A. K. analyzed the data; A. S. took the AFM imaging; R. H., W. M., Y. Z. helped with the schematic preparation and sample optimization. A. S. and Y. L. drafted the manuscript and all authors contributed to the manuscript.

Supplementary Information

All additional data and supporting information and methods are presented in the supplementary information file.

Acknowledgements

We would like to acknowledge the financial support from ANU PhD student scholarship, China Scholarship Council, Australian Research Council, ANU Major Equipment Committee fund, National Natural Science Foundation of China. We would also like to thank Professor Chennupati Jagadish and Professor Barry Luther-Davies from the Australian National

University for their facility support.

Competing financial interests

The authors declare that they have no competing financial interests.

Table of Content (TOC) graphic

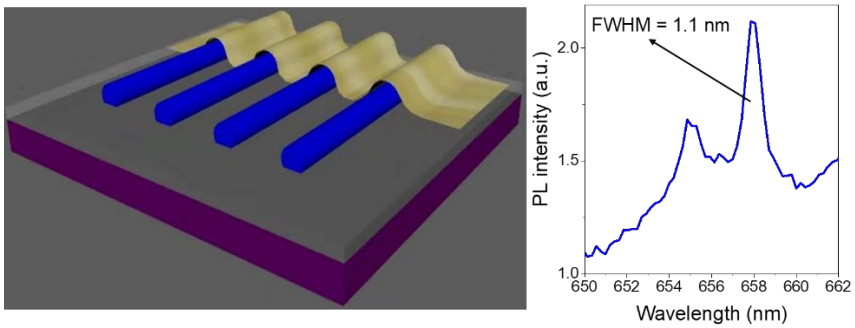

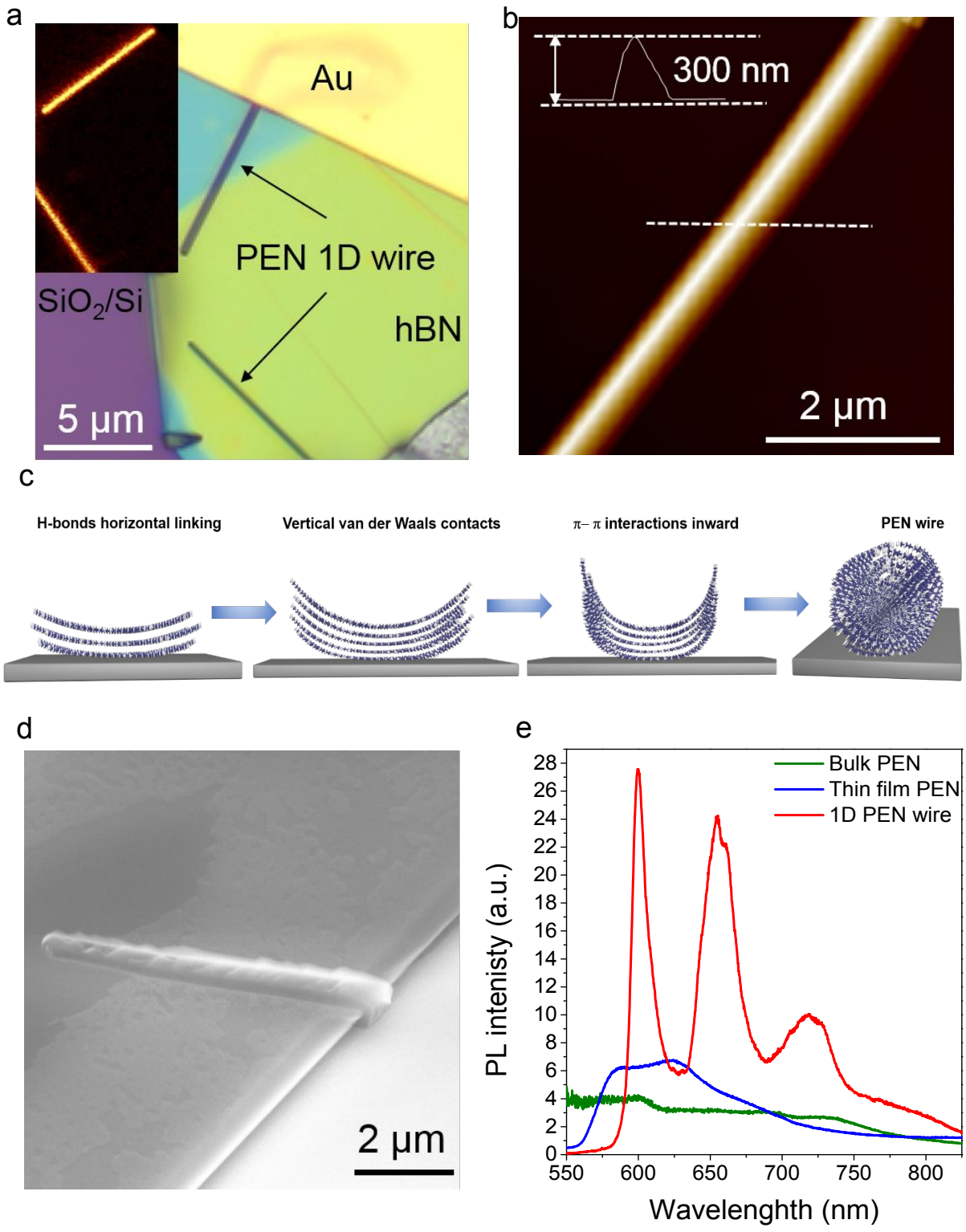

Figure 1 | Characterization of PEN wires a, Optical microscope image of the quasi 1D PEN wires used for measurements. The scale bar is 5 μm. Inset: PL mapping image of the PEN wires showing the strong emission from wires. **b**, Zoomed Atomic force microscope (AFM) image of the PEN wires confirming the diameter to be ~ 300 nm. **c**, Schematic representation of the

growth mechanism of the PEN wires during the vapor deposition mechanism. See text for details. **d**, SEM image of the PVD grown PEN wires on hBN substrate, showing the morphology of the wire. **e**, PL emission spectra (red curve) from PEN wires at room temperature, showing three clear peaks at 600 nm, 660 nm and 730 nm. Broad sideband PL emission from bulk (green) and thin film crystalline pentacene grown on hBN (blue) is also shown for comparison.

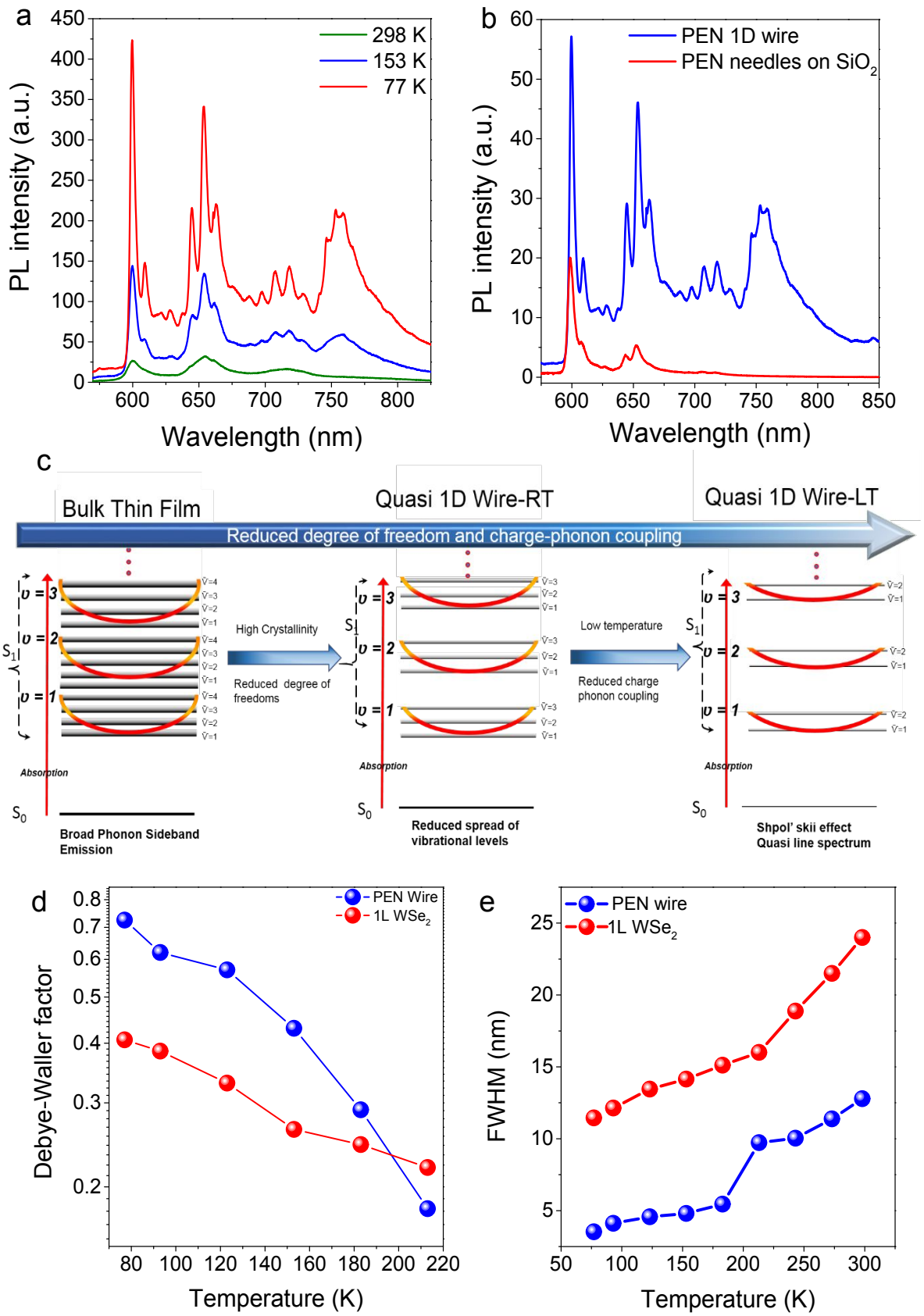

Figure 2 | Temperature dependent PL emission and Shpol' skii effect. a, Measured PL spectra at various temperatures from PEN wires. The vibronic levels are well resolvable at cryogenic temperatures as evident from quasi-line spectral emissions. **b**, PL emission spectra

comparison between PEN wires grown on hBN with PEN needles grown in SiO_2 at 77 K. The PEN needles on SiO_2 do not show the clearly resolvable vibronic levels as shown from PEN wires grown on hBN. **c**, Schematic showing the energy level diagram in pentacene. The exciton bands with vibrational coupling for pentacene thin film (left) are shown. Only first three vibronic bands are shown. The vibronic bands (red) are demonstrated by υ =1, 2, 3... and the vibrational bands (grey) formed due to strong coupling between the exciton and phonons are shown by $\grave{\nu}$=1,2,3… The spread or thickness of vibrational levels accounts for the level of phononic coupling and degree of freedom in all cases. The molecules in bulk thin film case are at various energy levels leading to an emission band broadening and the PL emission is a broad sideband phononic emission as shown in Figure1d. The vibronic levels in PEN wires at RT are further resolved due to confinement of molecules distinctly in the lattice with specific geometric configuration and high degree of orientation. In this case more neighboring molecules have similar energy levels, leading to a degenerate PL emission spectrum as shown in Figure1d. At low temperature (right), the charge-phonon coupling, or vibrational coupling is further reduced leading to even further reduced thickness of vibrational levels at low temperature. As result the vibronic levels are well defined due to reduced degree of freedom of molecules and minimal charge-phonon coupling. This effect of observing quasi-line spectra at low temperature is called Shpol' skii effect as shown in Figure2a. **d**, Debye-Waller (*DW*) factor obtained from PEN wire (peak =600 nm) and 1L WSe_2 (peak =750nm) as a function of the temperature. At 77 K the D*W* factor is much higher in PEN wires as compared to TMDC monolayers confirming an almost zero phonon emission or a quasi-linear PL emission. **e**, Variation of full-width half maximum (FWHM) of excitonic PL emission peaks from PEN wires(peak = 600nm) and WSe_2 (peak =750 nm). The FWHM from PEN wire excitonic emission is much lower as compared to TMD monolayer and the reduction in FWHM with temperature to ~ 3nm, confirms the zero-phonon line emission from PEN wires.

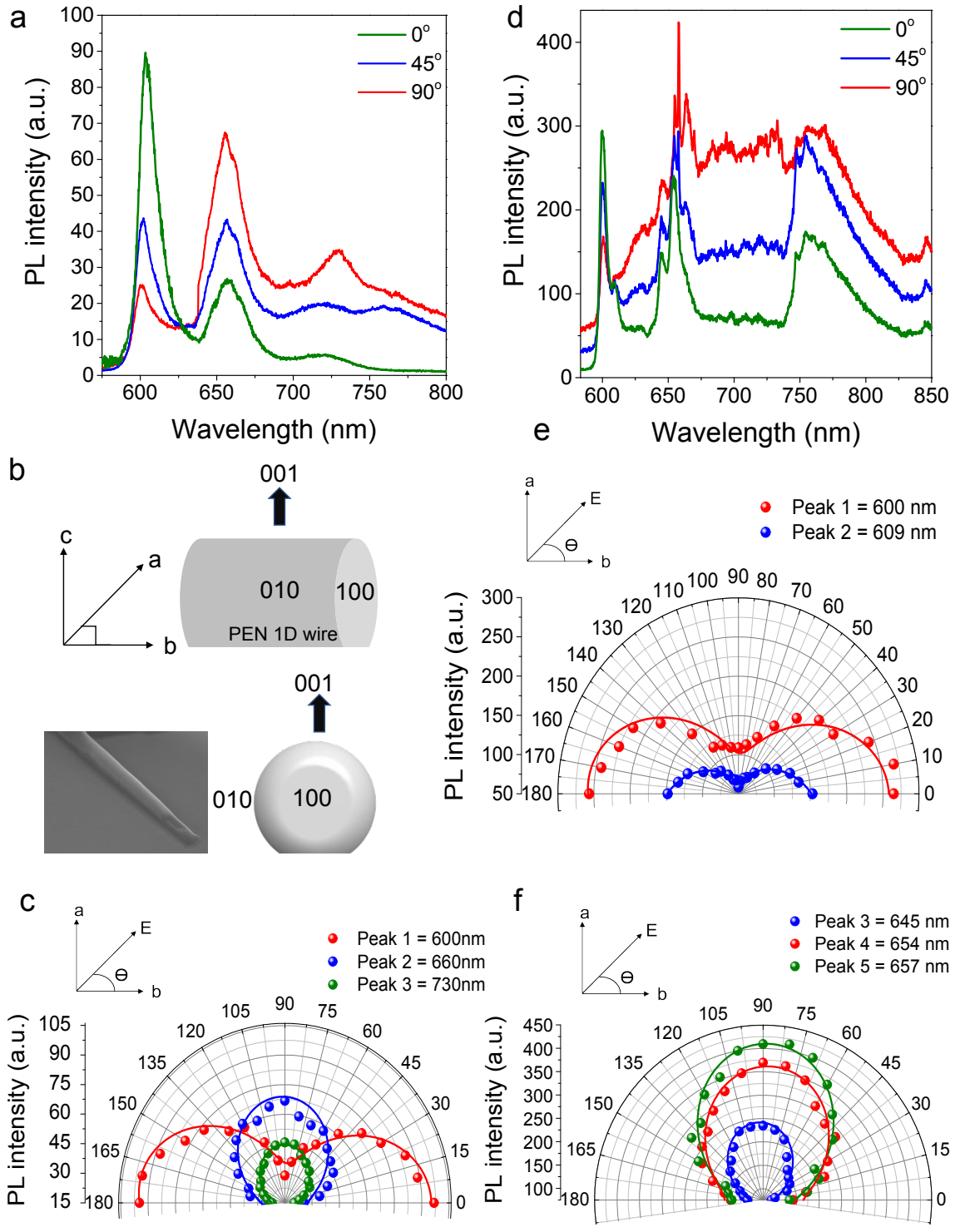

Figure 3 | Polarization angle-dependent PL measurements. a, Measured PL intensity as a function of emission polarization angle θ from PEN wire samples at room temperature, revealing the anisotropic excitonic nature of emission from the PEN wires. In experiment, the excitation polarization angle was fixed and the polarization angle of the emission θ was determined by using an angle-variable polarizer located in front of the detector. **b**, Schematic diagram showing the growth morphology and crystalline structure molecular arrangement in PEN wires grown on hBN. The molecular axis as in a conventional triclinic pentacene crystal

have been marked as a, b and c. The inset SEM image shows the 001 and 100 face of as grown PEN wires. **c**, Measured polar plot of PL emission spectra peaks as a function of emission polarization angle θ from PEN wires at room temperature revealing the opposite anisotropic excitonic nature of PL emission peaks at 600 nm, 660 nm and 730 nm. E is the direction of selected emission polarization. 'a' and 'b' are pentacene molecular axis. **d**, Measured PL intensity as a function of emission polarization angle θ from PEN wire samples at 77 K. **e-f**, Measured polar plot of PL emission spectra peaks as a function of emission polarization angle θ from PEN wires at 77 K revealing the opposite anisotropic excitonic nature of PL emission peaks. For remaining polar plots see Figure S13.

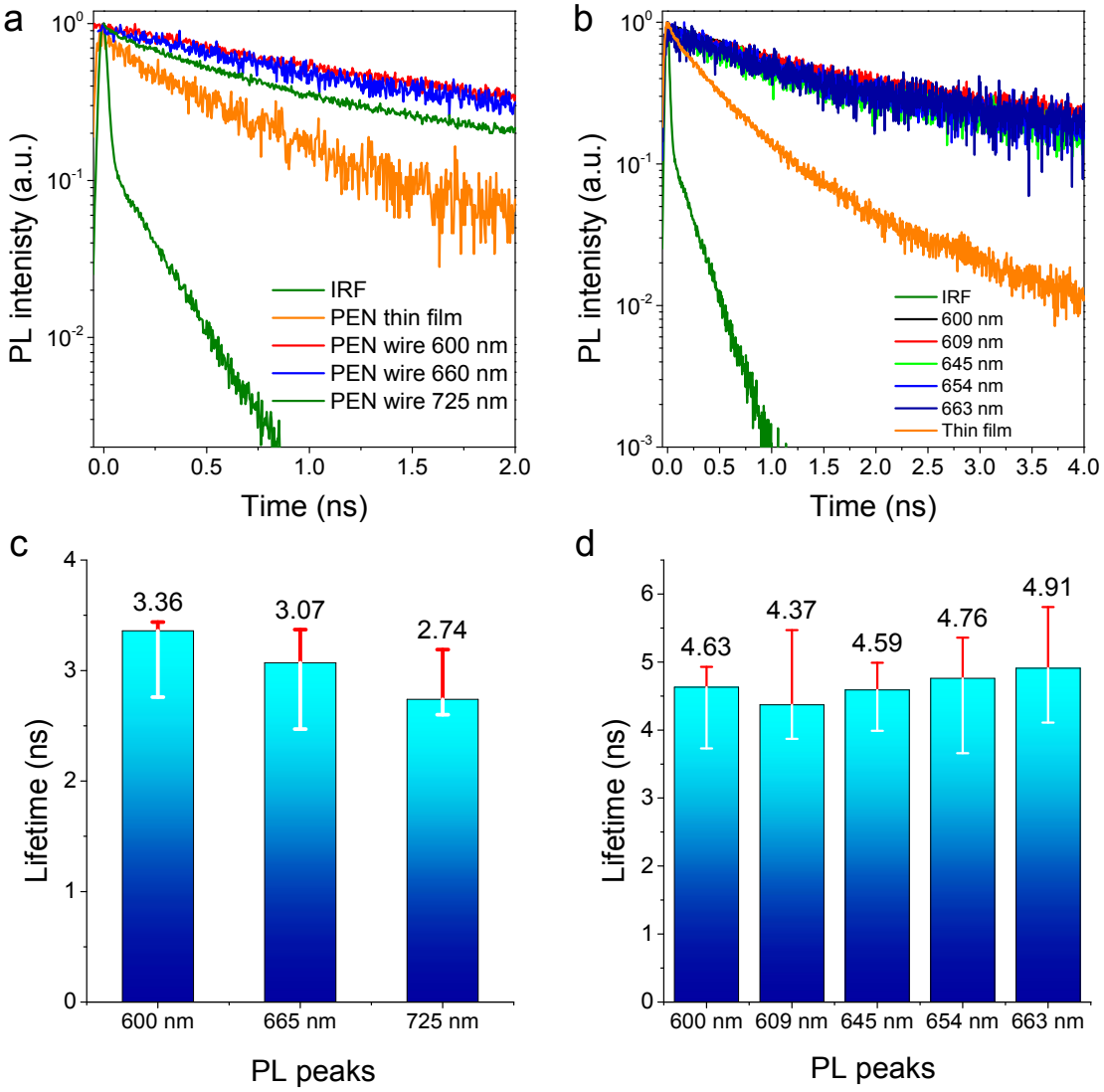

Figure 4 | Time-resolved PL emission from PEN wires. a-b, Time-resolved PL emission (normalized) from PEN wires at 298 K (a) and 77 K (b). The orange curve represents the decay curve from bulk thin film pentacene for comparison. An effective long lifetime of 1.24 ns (1.01 ns) was extracted from the orange decay curve at 298 K (77 K), by a fitting with deconvolution using the instrument response function (IRF) (green curve). The red/blue balls represent decay curve from 1L, which is from FR exciton emission. The red (600 nm), blue (660 nm) and green (730 nm) decay curves are from PEN wires PL emission spectra. The deconvolution using IRF, gives an effective lifetime value of 3.36 ns, 3.07 ns and 2.74 ns respectively at 298 K. Similarly, at 77 K, deconvolution with IRF has been used to extract a long lifetime from various peaks at 77 K. See text for values**. c-d,** Graphical representation (with experimental errors bars) showing the distribution of extracted lifetime from various peaks of PL emission spectra from PEN wires. For peak positions refer to Table S2.

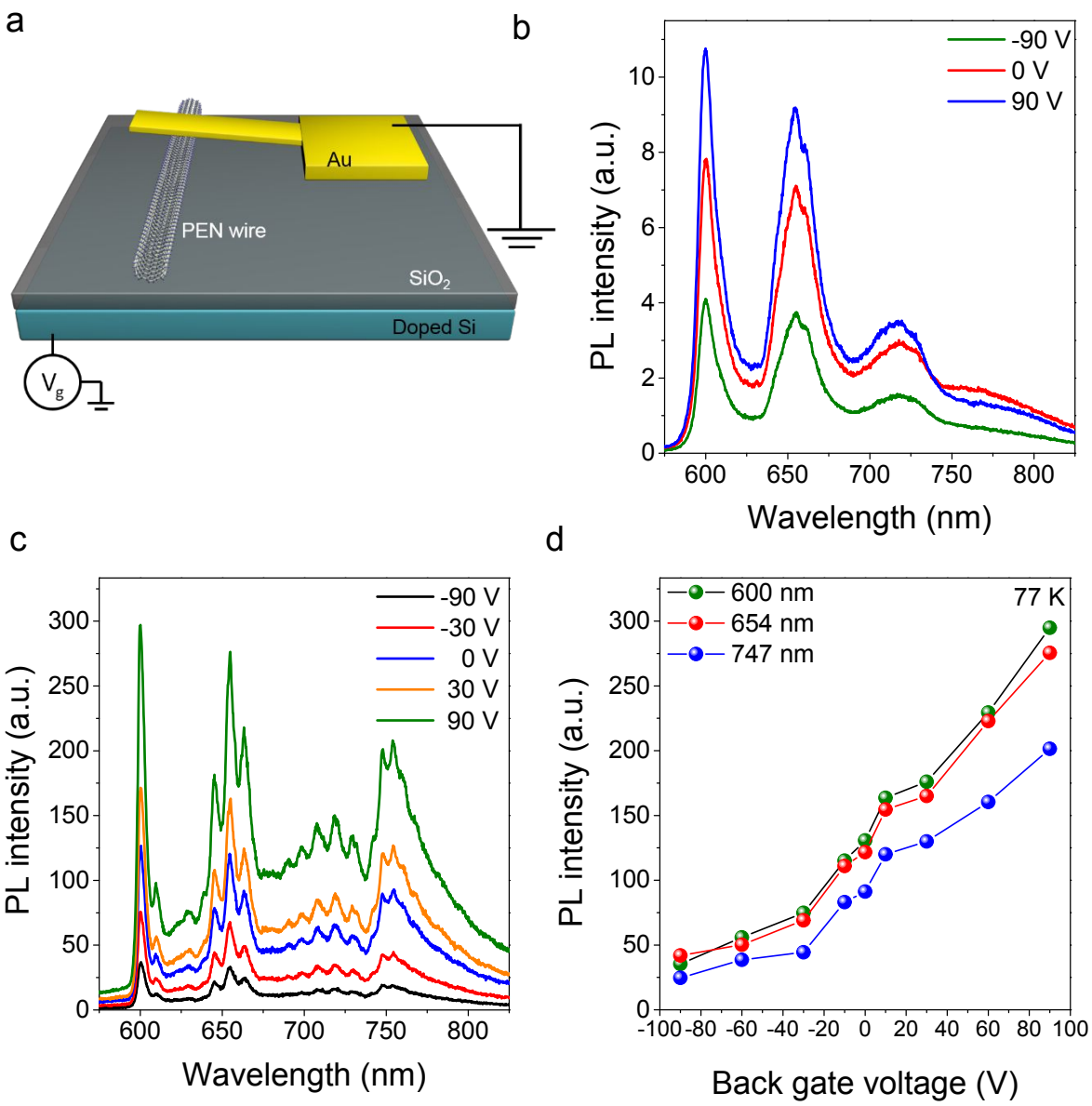

Figure 5 | Back gate dependent modulation of PL emission from PEN wire MOS device. **a,** Schematic diagram of the MOS device used for static doping of charges into the PEN wire. (See optical image in Figure1a). **b**, Measured PL spectra from PEN wire sample at room temperature under various back gate voltages, showing clear modulation of all emission peaks. **c**, Measured PL spectra from PEN wire sample at 77 K under various back gate voltages, showing similar modulation of all emission peaks as observed at room temperature. **d**, Variation of peak =600 nm, 654 nm and 747 nm as a function of sweeping back gate voltage at 77 K, demonstrating a clear n-type doping in the PEN wire. The MOS device confirms the external control of the PL emission that can be achieved by modulating back gate voltage.

References

1. Sild, O.; Haller, K., *Zero-Phonon Lines: And Spectral Hole Burning in Spectroscopy and Photochemistry*. Springer Science & Business Media: 2012.
2. Naumov, A. V., Low-temperature spectroscopy of organic molecules in solid matrices: from the Shpol'skii effect to laser luminescent spectromicroscopy for all effectively emitting single molecules. *Physics-Uspekhi* **2013,** *56* (6), 605-622.
3. Kiraz, A.; Ehrl, M.; Mustecaplioglu, O.; Hellerer, T.; Brauchle, C.; Zumbusch, A. In *Zero-phonon-line emission of single molecules for applications in quantum information processing*, Photonic Materials, Devices, and Applications, International Society for Optics and Photonics: 2005; pp 584-592.
4. Zhao, Y. S.; Peng, A.; Fu, H.; Ma, Y.; Yao, J., Nanowire waveguides and ultraviolet lasers based on small organic molecules. *Advanced Materials* **2008,** *20* (9), 1661-1665.
5. O'carroll, D.; Lieberwirth, I.; Redmond, G., Microcavity effects and optically pumped lasing in single conjugated polymer nanowires. *Nature nanotechnology* **2007,** *2* (3), 180.
6. Zhao, Y. S.; Xu, J.; Peng, A.; Fu, H.; Ma, Y.; Jiang, L.; Yao, J., Optical waveguide based on crystalline organic microtubes and microrods. *Angewandte Chemie International Edition* **2008,** *47* (38), 7301-7305.
7. Zhao, Y. S.; Fu, H.; Peng, A.; Ma, Y.; Liao, Q.; Yao, J., Construction and optoelectronic properties of organic one-dimensional nanostructures. *Accounts of chemical research* **2009,** *43* (3), 409-418.
8. Law, M.; Sirbuly, D. J.; Johnson, J. C.; Goldberger, J.; Saykally, R. J.; Yang, P., Nanoribbon waveguides for subwavelength photonics integration. *Science* **2004,** *305* (5688), 1269-1273.
9. Zhao, Y. S.; Fu, H.; Hu, F.; Peng, A.; Yang, W.; Yao, J., Tunable emission from binary organic one-dimensional nanomaterials: an alternative approach to white-light emission. *Advanced Materials* **2008,** *20* (1), 79-83.
10. Zhao, Y. S.; Fu, H.; Hu, F.; Peng, A. D.; Yao, J., Multicolor emission from ordered assemblies of organic 1D nanomaterials. *Advanced Materials* **2007,** *19* (21), 3554-3558.
11. Bree, P. d.; Wiersma, D. A., Application of Redfield theory to optical dephasing and line shape of electronic transitions in molecular mixed crystals. *The Journal of Chemical Physics* **1979,** *70* (2), 790-801.
12. Rebane, K. K., Zero-phonon line as the foundation stone of high-resolution matrix spectroscopy, persistent spectral hole burning, single impurity molecule spectroscopy. *Chemical Physics* **1994,** *189* (2), 139-148.
13. Shpol'skiĭ, É. V., LINE FLUORESCENCE SPECTRA OF ORGANIC COMPOUNDS AND THEIR APPLICATIONS. *Soviet Physics Uspekhi* **1960,** *3* (3), 372-389.
14. Zhao, Y. S.; Xiao, D.; Yang, W.; Peng, A.; Yao, J., 2, 4, 5-Triphenylimidazole nanowires with fluorescence narrowing spectra prepared through the adsorbent-assisted physical vapor deposition method. *Chemistry of materials* **2006,** *18* (9), 2302-2306.
15. Xiao, S.; Tang, J.; Beetz, T.; Guo, X.; Tremblay, N.; Siegrist, T.; Zhu, Y.; Steigerwald, M.; Nuckolls, C., Transferring self-assembled, nanoscale cables into electrical devices. *Journal of the American Chemical Society* **2006,** *128* (33), 10700-10701.
16. Berson, S.; De Bettignies, R.; Bailly, S.; Guillerez, S., Poly (3-hexylthiophene) fibers for photovoltaic applications. *Advanced Functional Materials* **2007,** *17* (8), 1377-1384.
17. Merlo, J. A.; Frisbie, C. D., Field effect transport and trapping in regioregular polythiophene nanofibers. *The Journal of Physical Chemistry B* **2004,** *108* (50), 19169-19179.
18. Kim, D.; Han, J. T.; Park, Y.; Jang, Y.; Cho, J.; Hwang, M.; Cho, K., Single-crystal polythiophene microwires grown by self-assembly. *Advanced Materials* **2006,** *18* (6), 719-723.

19. Briseno, A. L.; Mannsfeld, S. C.; Jenekhe, S. A.; Bao, Z.; Xia, Y., Introducing organic nanowire transistors. *Materials Today* **2008,** *11* (4), 38-47.
20. Schenning, A. P.; Meijer, E., Supramolecular electronics; nanowires from self-assembled π-conjugated systems. *Chemical Communications* **2005,** (26), 3245-3258.
21. Fu, H.; Xiao, D.; Yao, J.; Yang, G., Nanofibers of 1, 3-diphenyl-2-pyrazoline induced by cetyltrimethylammonium bromide micelles. *Angewandte Chemie International Edition* **2003,** *42* (25), 2883-2886.
22. Hu, J.-S.; Guo, Y.-G.; Liang, H.-P.; Wan, L.-J.; Jiang, L., Three-dimensional self-organization of supramolecular self-assembled porphyrin hollow hexagonal nanoprisms. *Journal of the American Chemical Society* **2005,** *127* (48), 17090-17095.
23. Kang, L.; Chen, Y.; Xiao, D.; Peng, A.; Shen, F.; Kuang, X.; Fu, H.; Yao, J., Organic core/diffuse-shell nanorods: fabrication, characterization and energy transfer. *Chemical Communications* **2007,** (26), 2695-2697.
24. An, B. K.; Kwon, S. K.; Park, S. Y., Photopatterned arrays of fluorescent organic nanoparticles. *Angewandte Chemie* **2007,** *119* (12), 2024-2028.
25. An, B.-K.; Kwon, S.-K.; Jung, S.-D.; Park, S. Y., Enhanced emission and its switching in fluorescent organic nanoparticles. *Journal of the American Chemical Society* **2002,** *124* (48), 14410-14415.
26. Lloyd, M. T.; Anthony, J. E.; Malliaras, G. G., Photovoltaics from soluble small molecules. *Materials Today* **2007,** *10* (11), 34-41.
27. Shin, T. J.; Yang, H.; Ling, M.-m.; Locklin, J.; Yang, L.; Lee, B.; Roberts, M. E.; Mallik, A. B.; Bao, Z., Tunable thin-film crystalline structures and field-effect mobility of oligofluorene–thiophene derivatives. *Chemistry of Materials* **2007,** *19* (24), 5882-5889.
28. DeLongchamp, D. M.; Kline, R. J.; Lin, E. K.; Fischer, D. A.; Richter, L. J.; Lucas, L. A.; Heeney, M.; McCulloch, I.; Northrup, J. E., High carrier mobility polythiophene thin films: structure determination by experiment and theory. *Advanced Materials* **2007,** *19* (6), 833-837.
29. Spano, F. C., The Spectral Signatures of Frenkel Polarons in H- and J-Aggregates. *Accounts of Chemical Research* **2010,** *43* (3), 429-439.
30. Woo, H. Y.; Liu, B.; Kohler, B.; Korystov, D.; Mikhailovsky, A.; Bazan, G. C., Solvent Effects on the Two-Photon Absorption of Distyrylbenzene Chromophores. *Journal of the American Chemical Society* **2005,** *127* (42), 14721-14729.
31. Park, J. E.; Son, M.; Hong, M.; Lee, G.; Choi, H. C., Crystal-Plane-Dependent Photoluminescence of Pentacene 1D Wire and 2D Disk Crystals. *Angewandte Chemie* **2012,** *124* (26), 6489-6494.
32. Bloess, A.; Durand, Y.; Matsushita, M.; Verberk, R.; Groenen, E. J. J.; Schmidt, J., Microscopic Structure in a Shpol'skii System: A Single-Molecule Study of Dibenzanthanthrene in n-Tetradecane. *The Journal of Physical Chemistry A* **2001,** *105* (13), 3016-3021.
33. Kizel, V. A.; Sapozhnikov, M. N., The Interaction of Impurity Centres with the Surroundings and Quasi-Line Spectra. *physica status solidi (b)* **1970,** *41* (1), 207-216.
34. Tokousbalides, P., Observation of quasilinear fluorescence spectra (the "Shpol'skii effect") in matrix-isolated polycyclic aromatic hydrocarbons. *Journal of physical chemistry (1952) 81* (18), 1769-1772.
35. Zhang, W.; Yan, Y.; Gu, J.; Yao, J.; Zhao, Y. S., Low-Threshold Wavelength-Switchable Organic Nanowire Lasers Based on Excited-State Intramolecular Proton Transfer. *Angewandte Chemie International Edition* **2015,** *54* (24), 7125-7129.
36. Muccini, M., A bright future for organic field-effect transistors. *Nature Materials* **2006,** *5*, 605.
37. Duan, X.; Huang, Y.; Agarwal, R.; Lieber, C. M., Single-nanowire electrically driven

lasers. *Nature* **2003,** *421*, 241.
38. Anthony, J. E., Functionalized Acenes and Heteroacenes for Organic Electronics. *Chemical Reviews* **2006,** *106* (12), 5028-5048.
39. Zhang, Y.; Qiao, J.; Gao, S.; Hu, F.; He, D.; Wu, B.; Yang, Z.; Xu, B.; Li, Y.; Shi, Y.; Ji, W.; Wang, P.; Wang, X.; Xiao, M.; Xu, H.; Xu, J.-B.; Wang, X., Probing Carrier Transport and Structure-Property Relationship of Highly Ordered Organic Semiconductors at the Two-Dimensional Limit. *Physical Review Letters* **2016,** *116* (1), 016602.
40. Spano, F. C., Optical microcavities enhance the exciton coherence length and eliminate vibronic coupling in J-aggregates. *The Journal of Chemical Physics* **2015,** *142* (18), 184707.
41. Beljonne, D.; Yamagata, H.; Brédas, J. L.; Spano, F. C.; Olivier, Y., Charge-Transfer Excitations Steer the Davydov Splitting and Mediate Singlet Exciton Fission in Pentacene. *Physical Review Letters* **2013,** *110* (22), 226402.
42. Yamagata, H.; Spano, F. C., Strong Photophysical Similarities between Conjugated Polymers and J-aggregates. *The Journal of Physical Chemistry Letters* **2014,** *5* (3), 622-632.
43. McCumber, D. E.; Sturge, M. D., Linewidth and Temperature Shift of the R Lines in Ruby. *Journal of Applied Physics* **1963,** *34* (6), 1682-1684.
44. Silsbee, R. H., Thermal Broadening of the M\"ossbauer Line and of Narrow-Line Electronic Spectra in Solids. *Physical Review* **1962,** *128* (4), 1726-1733.
45. Sears, V. F., Debye–Waller factor for elemental crystals. *Acta crystallographica. Section A, Foundations of crystallography 47* (4), 441-446.
46. Vainer, Y. G.; Kol'chenko, M. A.; Naumov, A. V.; Personov, R. I.; Zilker, S. J., Photon echoes in doped organic amorphous systems over a wide (0.35–50K) temperature range. *Journal of Luminescence* **2000,** *86* (3), 265-272.
47. Briseno, A. L.; Mannsfeld, S. C. B.; Reese, C.; Hancock, J. M.; Xiong, Y.; Jenekhe, S. A.; Bao, Z.; Xia, Y., Perylenediimide Nanowires and Their Use in Fabricating Field-Effect Transistors and Complementary Inverters. *Nano Letters* **2007,** *7* (9), 2847-2853.
48. Debije, M. G.; Chen, Z.; Piris, J.; Neder, R. B.; Watson, M. M.; Müllen, K.; Würthner, F., Dramatic increase in charge carrier lifetime in a liquid crystalline perylene bisimide derivative upon bay substitution with chlorine. *Journal of Materials Chemistry* **2005,** *15* (12), 1270-1276.
49. Aghaei, E.; Haghighi, M., Enhancement of catalytic lifetime of nanostructured SAPO-34 in conversion of biomethanol to light olefins. *Microporous and Mesoporous Materials* **2014,** *196*, 179-190.
50. Palummo, M.; Bernardi, M.; Grossman, J. C., Exciton radiative lifetimes in two-dimensional transition metal dichalcogenides. *Nano letters* **2015,** *15* (5), 2794-2800.
51. Liang, Q.; Liu, J.; Cheng, Z.; Li, Y.; Chen, L.; Zhang, R.; Zhang, J.; Han, Y., Enhancing the crystallization and optimizing the orientation of perovskite films via controlling nucleation dynamics. *Journal of Materials Chemistry A* **2016,** *4* (1), 223-232.
52. Shao, S.; Dong, J.; Duim, H.; Gert, H.; Blake, G. R.; Portale, G.; Loi, M. A., Enhancing the crystallinity and perfecting the orientation of formamidinium tin iodide for highly efficient Sn-based perovskite solar cells. *Nano Energy* **2019,** *60*, 810-816.